

AD-A042 484

WESTINGHOUSE ELECTRIC CORP PITTSBURGH PA RESEARCH A--ETC F/G 20/5  
COPPER HALIDE LASER RESEARCH. (U)  
MAR 77 C S LIU, D W FELDMAN, J L PACK

N00014-74-C-0445  
NL

UNCLASSIFIED

| OF |  
AD  
A042484



ADA 042484

12 J

COPPER HALIDE LASER RESEARCH

FINAL REPORT

Contract No. N00014-74-C-0445 (ONR)

C. S. Liu, D. W. Feldman, J. L. Pack and L. A. Weaver  
Westinghouse R&D Center  
Pittsburgh, Pennsylvania 15235

March 31, 1977

DDC  
RECEIVED  
JUL 28 1977  
E

AD No. \_\_\_\_\_  
DDC FILE COPY.

DISTRIBUTION STATEMENT A  
Approved for public release;  
Distribution Unlimited

APPROVED FOR PUBLIC RELEASE: DISTRIBUTION UNLIMITED

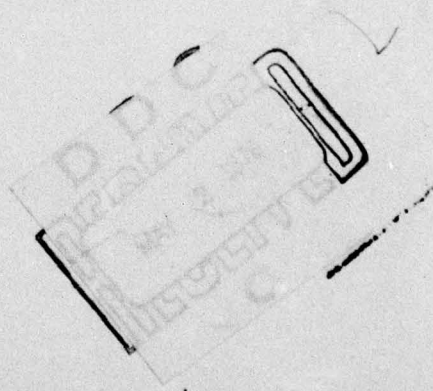
⑥ COPPER HALIDE LASER RESEARCH

⑨ FINAL REPORT

⑮ Contract No. N00014-74-C-0445 (ONR) *new*

⑩ C. S. / Liu, D. W. / Feldman, J. L. / Pack  L. A. / Weaver  
Westinghouse R&D Center  
Pittsburgh, Pennsylvania 15235

⑫ 42p.



ACQUISITION FOR	
NTIS	Whole Section <input checked="" type="checkbox"/>
DOC	Buff Section <input type="checkbox"/>
ANNOUNCED	<input type="checkbox"/>
JUSTIFICATION	<del> </del>
BY	
DISTRIBUTION/AVAILABILITY US G	
A	

⑪ 31 Mar  1977

376 625

LB

TABLE OF CONTENTS

	<u>Page</u>
SUMMARY . . . . .	1
1. INTRODUCTION . . . . .	2
1.1 Copper Laser Background . . . . .	2
1.2 Copper Vapor Laser Characteristics . . . . .	4
1.3 Copper Vapor Generation . . . . .	9
1.4 Copper Vapor Excitation Processes . . . . .	11
1.5 Laser Energy Output Scaling . . . . .	14
1.5.1 Energy Density Scaling . . . . .	15
1.5.2 Volume Scaling . . . . .	15
2. EXPERIMENTAL RESULTS . . . . .	17
2.1 Design and Fabrication of High Power Laser Tubes . . . . .	17
2.2 Design and Fabrication of the Electrical Pulsing Unit . . . . .	17
2.3 Laser Operating Characteristics . . . . .	22
2.3.1 Small Bore Tubes . . . . .	22
2.3.2 Large Bore Tubes . . . . .	26
2.4 Absorption Apparatus . . . . .	28
2.5 Lifetime Limitations and Tube Configurations . . . . .	32
3. CONCLUSIONS AND RECOMMENDATIONS . . . . .	33
4. REFERENCES . . . . .	37

## LIST OF FIGURES

		<u>Page</u>
Figure 1.1	Energy level diagram for the copper I ( $1S$ core configuration only).	6
Figure 1.2	Effective transition lifetimes for a copper laser system without and with resonance radiation trapping.	7
Figure 1.3	Equilibrium copper vapor density as a function of temperature.	10
Figure 1.4	Maximum available copper atom density as a function of temperature for various trimeric copper halides.	12
Figure 2.1	Basic pulser circuit.	19
Figure 2.2	Pulser circuit waveforms.	19
Figure 2.3	Waveforms of existing pulser.	20
Figure 2.4	Specific output energy as a function of wall temperature for a double-pulsed copper bromide laser.	23
Figure 2.5	Specific output energy as a function of excitation pulse delay for a double-pulsed copper bromide laser.	24
Figure 2.6	Typical output pulse waveform.	25
Figure 2.7	Experimental absorption apparatus.	30
Figure 2.8	Apparatus for absorption measurements.	31

## SUMMARY

This report describes results of experimental studies of copper halide laser systems. The properties of double-pulse and multipulse copper halide laser systems have been established. Both pulser and laser tube designs have demonstrated reliable operation under high power, high prf operation: pulser lifetimes of 300 hours and laser tube lifetimes of 100 hours without failure have been recorded for self-heated, high power operation. Laser tubes of various sizes were tested for high energy per pulse operation; the results indicated that high energy operation is presently inhibited by discharge stability problems which occurred in scaled-up laser tubes, and that optimum prf for multipulse excitation does not vary with tube diameter over the range studied.

This study recommends the future directions for further activities in copper halide laser research. The first is to recognize the inherent advantages of copper halide lasers at high prf operation for high average power and efficiency. This feature coupled with the demonstrated seal-off, self-heated and long-lived tube characteristics, render the copper halide laser especially attractive for applications where reliable, high prf, high average power laser sources are required. Evidently the low prf, high energy per pulse does not favor the best operating features of these lasers.

The second recommendation is that practical solutions to the discharge stability problem in copper halide lasers should be developed in order to realize the full promise of high specific output energies in larger tube embodiments. Various forms of transverse discharge offer considerable promise for solving this problem. Of course, the technological difficulties of high temperature operation are considerable. However, the laser performance improvements to be realized by overcoming discharge stability limitations are substantial, and amply justify the required development effort.

## I. INTRODUCTION

The main objective of this research program was to develop a high energy per pulse copper halide laser system operating at a low prf with a long operating lifetime, and to establish the critical physical processes and engineering considerations relevant to scaling the present system up to the 50 mJ per pulse level. In order to accomplish these goals, laser discharge tubes with various lengths and diameters were fabricated and tested, and the operating characteristics of the double-pulsed and continuously pulsed copper halide laser were measured.

These measurements have provided the information required to recommend a framework for the future development of copper halide laser systems.

### 1.1 Copper Laser Background

Laser emission from the copper atom was first reported by Walter et al.<sup>1,2</sup> in 1966. In this early work, 5106 Å and 5782 Å laser outputs were obtained from pulsed longitudinal discharges in pure copper at temperatures of about 1500°C, with conversion efficiencies of about 0.1%. In subsequent work, Walter<sup>3</sup> demonstrated average power levels as high as 0.5 W at pulse repetition rates of 1 kHz, with the conversion efficiency being greater than 1%. But despite these encouraging demonstrations of efficient, visible laser operation, no substantial improvements in the copper laser technology were forthcoming until 1972.

In that year Isaev, Kazaryan and Petrash<sup>4</sup> disclosed average power levels of 15 W at pulse repetition rates of 18 kHz in pure copper lasers operating at 1500°C. These performance figures were achieved with an overall efficiency of 1%, and the waste heat from the discharge was employed to heat the tube.

The Russian experiments at the 15 W level encouraged many fresh attempts to realize improved performance from copper lasers. Among these were supersonic expansion of copper vapor with transverse

electrical excitation,<sup>5</sup> heat pipe configurations for containing the copper vapor,<sup>6</sup> electron beam excitation of evaporated copper,<sup>7</sup> and self-heated slotted hollow cathode discharges in copper.<sup>8</sup> Each of these approaches has been successful in demonstrating laser feasibility.

Significant progress toward solving the high-temperature problem was reported by Weaver, Liu and Sucov<sup>9-11</sup> in 1973. Rather than employing pure copper as in previous approaches, the halides of copper were used at temperatures near 600°C. At these temperatures the copper halide vapor pressure is about 1 Torr, whereas pure copper vapor pressures of 1 Torr are obtained at about 1600°C. Superradiant laser emission at the copper 5106 Å and 5782 Å wavelengths was observed in pulsed CuI:Ar discharges contained within all-hot quartz envelopes. Copper laser emission was subsequently reported<sup>12</sup> in double-pulsed CuCl:He discharges, with optimum output occurring some 180 μsec after an initial preconditioning electrical discharge. These experiments demonstrated that copper laser emission could be obtained at substantially reduced operating temperatures, thereby greatly simplifying the materials, insulation, and lifetime considerations of pure copper lasers.

Recent experiments at the Westinghouse R&D Center<sup>13</sup> have increased the volumetric energy yield in CuI and CuBr lasers to 35 μJ cm<sup>-3</sup> in single 5106 Å/5782 Å laser pulses; this compares with 0.6 μJ cm<sup>-3</sup> obtained in the first experiments reported by Walter.<sup>2</sup> Furthermore, these experiments have demonstrated laser pulse repetition rates between 1 and 18 kHz, with optimum performance occurring near 5 kHz. Significantly, 5106 Å and 5782 Å laser pulses are obtained from each electrical excitation pulse. Apparently each discharge not only excites the copper atoms, but provides predissociation for the following discharge in the pulse train. This feature greatly simplifies the pulser requirements for copper halide lasers.

The problem of shortening the discharge pulse to times comparable to the copper laser pulse duration remains the major technical challenge in achieving efficient, high power operation. Copper halide devices produce 2.5 to 25 nsec laser pulse widths, and the laser output occurs within the first 20 nsec of the current pulse. Since

current pulses last for 100 to 200 nsec, most of the excitation pulse occurs after laser action has ceased. Thus higher efficiency operation will require improved energy storage, switching and discharge tube assemblies to minimize circuit inductance and thereby shorten the excitation pulse. In addition, the pulser unit must deliver its energy at a suitable repetition rate into a low-impedance discharge load, typically 5 to 10 ohms. This combination of electrical requirements represents a considerable challenge for the circuit designer.

Discharge stability is a problem in copper halide lasers, since the presence of electron-attaching species such as bromine tends to constrict the discharge into an arc. This tendency is more evident at higher operating temperatures and low prfs where greater concentrations of electronegative species are present. In fact, discharge stability considerations are likely the limiting factor determining the maximum operating temperatures and discharge cross section of the laser tube. The practical difficulty of initiating and maintaining diffuse glow discharges in electronegative gases is not to be underestimated and will limit the maximum useful copper halide densities.

### 1.2 Copper Vapor Laser Characteristics

Many of the operating characteristics of copper vapor lasers may be understood by examining the copper energy level diagram of Fig. 1.1. The copper ionization potential is only 7.72 eV, substantially lower than the 24.6 and 15.8 eV ionization potentials of He and Ar, respectively. Consequently the dominant electron production in typical copper lasers is through ionization of the copper rather than a buffer gas additive. Furthermore, the electronic levels of copper are the lowest-lying of the discharge species, so that most of the electronic excitation and fluorescence in copper lasers is associated with the copper species. The same comments apply to the halides of copper, since both ionization and fluorescence processes are dominated by the copper rather than the halides or their dissociated halogens. This property has been observed and employed for many years in both low

pressure and arc discharge lamps, where rare earth and metal halides are added to mercury:argon discharges to provide more pleasing color rendition through selected atomic fluorescence. This prior experience with metal halide lamps led Westinghouse in 1969 to study the possibility of reduced temperature copper laser operation through the use of copper halides.

The copper system is characterized by a spin-split doublet structure which results in a multiplicity of laser energy levels. As seen in Fig. 1.1, the  $4p^2P_{3/2}$  and  $4p^2P_{5/2}$  resonance levels are connected to the  $4s^2S_{1/2}$  ground state by 3248 Å and 3274 Å resonance transitions, respectively. The two resonance levels constitute the upper laser levels for the 5106 Å and 5782 Å laser transitions, and lie within  $248 \text{ cm}^{-1}$  of one another.<sup>14</sup> Since the mean thermal energy at 600°C is  $607 \text{ cm}^{-1}$ , these resonance levels likely exchange excitation energy quite rapidly during the current pulse. Furthermore, the 5700 Å ( $4p^2P_{3/2} \rightarrow 3d^9 4s^2 D_{3/2}$ ) transition originates on the 5106 Å upper laser level, but terminates on the 5782 Å lower laser level. All other known electronic transitions in copper originate from levels above the two resonance levels, and terminate on these resonance levels. The radiation from these higher-lying levels generally possesses the same relatively slow temporal characteristics as the discharge current, and has been attributed to afterglow recombination processes which populate the high-lying copper levels.<sup>11</sup>

The effective lifetimes of the  $4p^2P_{3/2}$  and  $4p^2P_{1/2}$  upper laser levels profoundly influence the copper laser kinetics, particularly near threshold conditions. When the copper ground state density  $N_1$  and tube radius  $R$  satisfy the condition  $N_1 R \gtrsim 10^{13} \text{ cm}^{-2}$ , the 3248 Å and 3274 Å resonance lines are imprisoned or trapped, thereby increasing the effective lifetimes of the resonance levels.<sup>10,11</sup> This effect is illustrated in the partial energy level diagrams of Fig. 1.4. Under these conditions the trapped lifetimes are 615 and 370 nsec for the  $4p^2P_{3/2}$  and  $4p^2P_{1/2}$  levels respectively, compared to 9.60 and 10.24 nsec without trapping. Thus the laser pumping requirements are greatly reduced for  $N_1 R \gtrsim 10^{13} \text{ cm}^{-2}$ ; this condition determines the effective minimum operating temperature for pure copper lasers as approximately 1200°C, and about 400°C for copper halide lasers. It also specifies



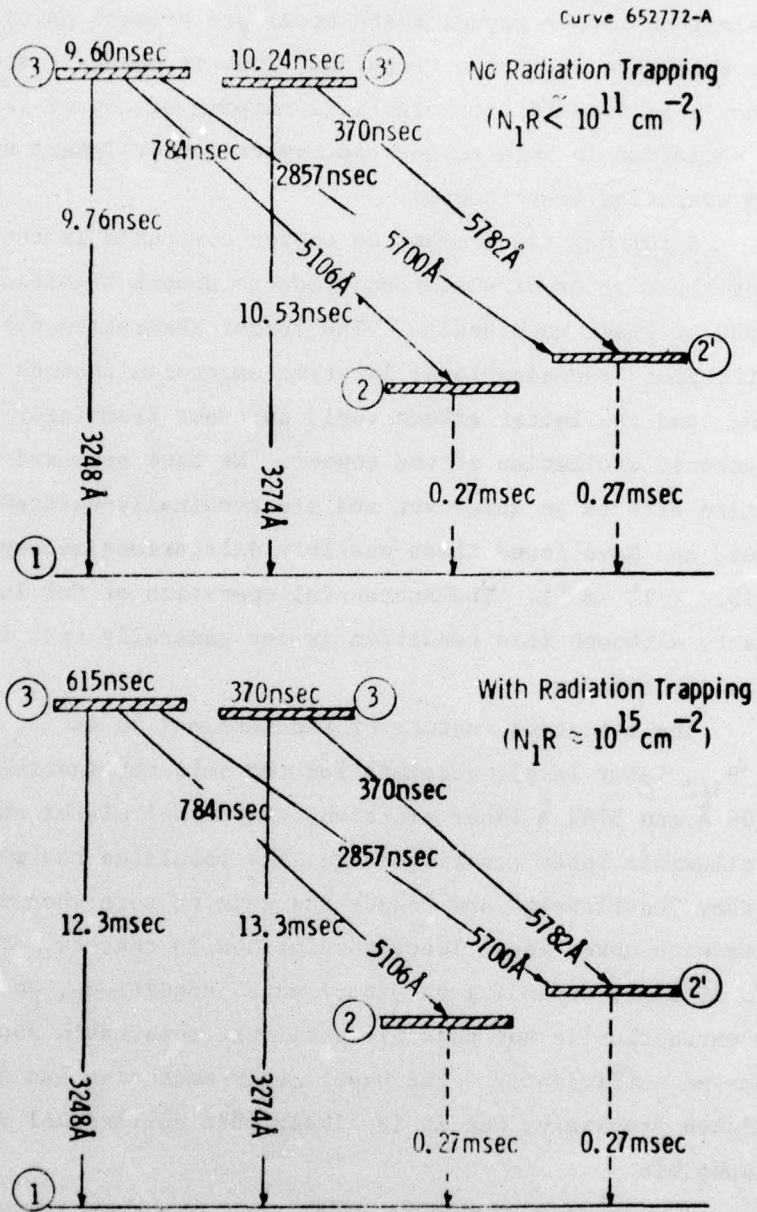


Fig. 1.2 - Effective transition lifetimes for a copper laser system without and with resonance radiation trapping

a minimum dissociation level in copper halide lasers at a given temperature, since no copper ground state atoms are present initially to provide resonance radiation trapping. Thus resonance trapping is a necessary condition for the practical pumping of copper lasers, and is easily satisfied in both copper and copper iodide lasers at their optimum operating temperatures.

A further requirement on copper compounds is that neither they nor their major dissociation products absorb significantly at the resonance or laser wavelengths. The former absorption effect would prevent copper resonance level lifetime extension through radiation trapping, and the latter effect would subtract from laser gain produced by electronic excitation of the copper. We have measured both of these absorption effects in quiescent and electronically-excited CuI:Ar mixtures, and have found these possibly deleterious absorptions to be negligible ( $<1\% \text{ cm}^{-1}$ ). The successful operation of CuI lasers confirms this fact, although this condition is not generally true in analogous metal halide systems.

The metastable nature of the terminal  $3d^9 4s^2 {}^2D_{5/2}$  and  $3d^9 4s^2 {}^2D_{3/2}$  laser levels accounts for the self-terminating nature of the 5106 Å and 5782 Å laser emission. Rapid stimulated emission of these allowable laser transitions quickly populates the metastables, which they "bottleneck" and reduce the gain to zero when approximate equality with upper laser level populations is reached. This occurs in 2 to 20 nsec, depending on experimental conditions, and further energy extraction is not possible until the metastable population has decayed sufficiently. The exact decay mechanism has not been established precisely, but it is likely that collisional deactivation is responsible.

The maximum available efficiency in pulsed copper lasers is derived from three factors: the ratio of laser energy to resonance radiation energy (63.6%), the ratio of the upper level degeneracy to the sum of upper and lower level degeneracies (60%), and the fraction of electrical input energy exciting the upper laser level (60%). The first factor is merely the quantum efficiency of the laser transition,

the second factor accounts for excited state energy remaining after "bottlenecking" of the metastable level, and the third factor is estimated in analogy with measured resonance level excitation efficiencies in mercury lamp discharges. Their product, 23%, is an effective upper bound for the laser conversion efficiency. The failure of existing devices to exceed even 1/20th of this efficiency is mainly due to temporal mismatch between excitation and laser pulses, inefficient resonance level excitation caused by insufficiently high values of E/N, and loss of population inversion by amplified spontaneous emission. Ionization, high-lying electronic level excitation, vibrational and rotational excitation, elastic processes, and dissociation can consume further energy. The extent to which these various factors degrade the efficiency is largely unknown, but it is clear that considerable increases in efficiency should be available by introducing certain power supply and optical design improvements.

### 1.3 Copper Vapor Generation

The class of metal lasers presents unique problems to the experimentalist, since metals possess negligible vapor pressure at room temperature. Copper is no exception, as the graph in Fig. 1.3 reveals. The minimum vapor densities required for resonance radiation trapping, namely  $\sim 10^{13} \text{ cm}^{-3}$  for typical 1 cm tube radii,<sup>11</sup> are not reached until temperatures near 1200°C are attained. Pure copper lasers typically operate between 1500 and 1700°C, where the corresponding copper vapor densities range between  $10^{15}$  and  $10^{16} \text{ cm}^{-3}$ . These high temperatures necessitate the use of materials such as alumina and tungsten, and invite severe problems in electrical insulation, chemical degradation, mechanical integrity and thermal economy. Since only a few transparent materials such as sapphire can withstand such temperatures, all pure copper lasers to date have operated with room-temperature optical windows. Thus an irreversible loss of copper occurs due to condensation near this cold region, thereby limiting the useful life of these devices. Furthermore, these high operating temperatures thermally populate the lower laser level. At 1500°C the copper metastable population is about 0.01%

Curve 658774-A

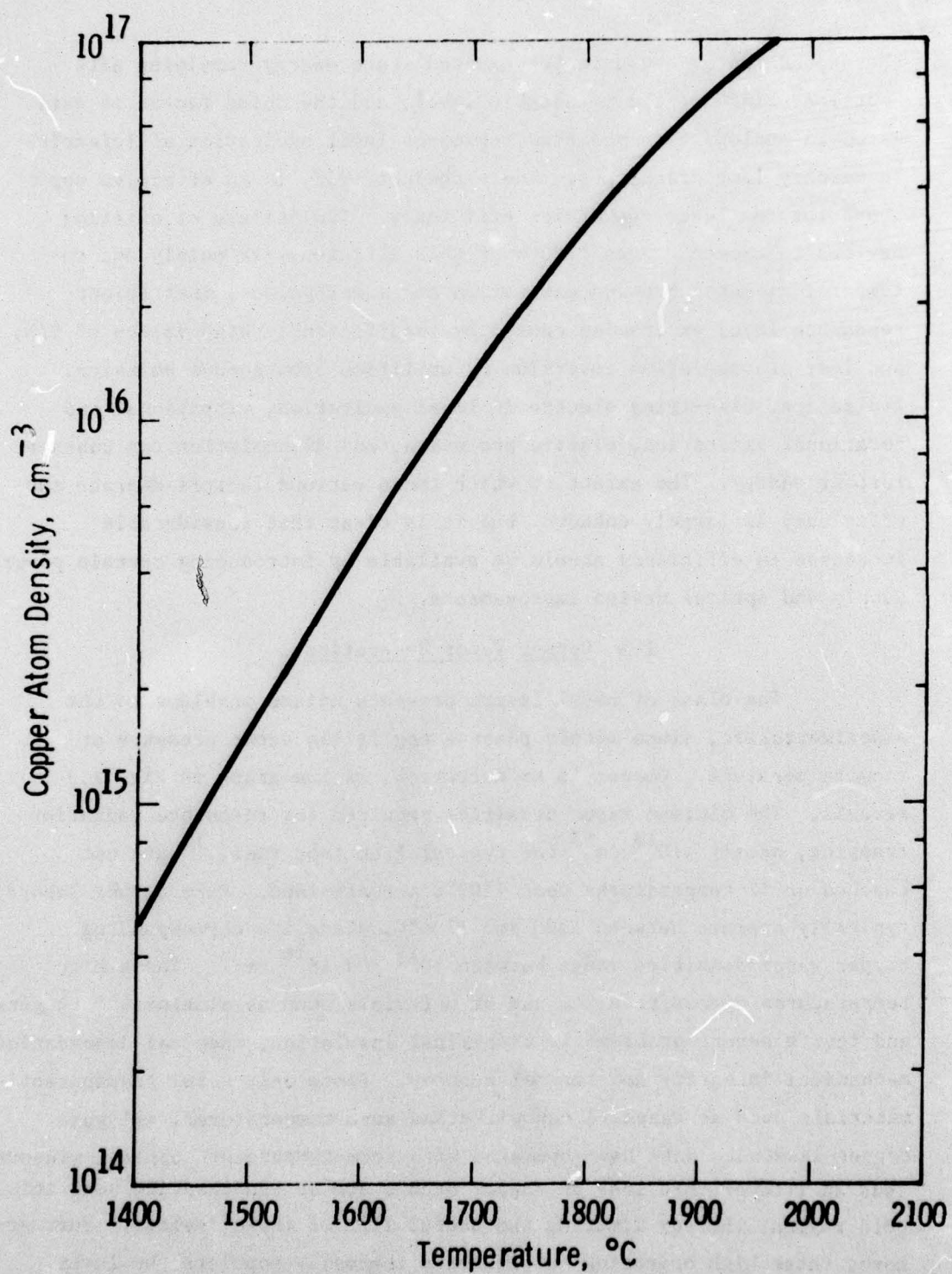


Fig. 1.3 - Equilibrium copper vapor density as a function of temperature

of the ground state population, but reaches about 0.1% at temperatures near 2000°C. This latter value is comparable to the fraction of atoms which can be excited to resonance levels in normal electrical discharges. Thus copper laser operation would not be expected beyond this temperature, which represents the practical upper material limit in any case. This restricts the available copper vapor density to a maximum of about  $10^{17}$  cm<sup>-3</sup>.

The search for volatile metal-bearing molecules in gas discharge lamp research has consistently uncovered only one satisfactory class of molecules, the metal halides. The copper halides volatilize primarily as trimeric molecules  $\text{Cu}_3\text{X}_3$ , where X stands for one of the halogen atoms, and attain vapor pressures near 1 Torr at temperatures of about 600°C. The maximum available copper atom density for various temperatures<sup>15</sup> is shown in Fig. 1.4 where it is assumed that each metal halide molecule carries three copper atoms. It is seen that threshold copper densities of  $10^{13}$  cm<sup>-3</sup> can be obtained at temperatures as low as 250°C for the chloride, assuming complete dissociation. Furthermore, copper densities greater than the maximum  $10^{17}$  cm<sup>-3</sup> attainable in pure copper at 2000°C are potentially available from the copper halides at temperatures beyond 600°C. Thus the copper halides provide copious amounts of copper, even assuming relatively low dissociation levels.

#### 1.4 Copper Vapor Excitation Processes

As discussed in Section 1.2, the copper halides do not absorb significantly at the copper resonance or laser wavelengths, and the copper atom is the dominant source of ionization and fluorescence. Moreover, the molecules are thermally stable over the temperature range of interest. But most important, the electrical decomposition within the discharge is reversible, with the original trimeric copper halide species being reformed from dissociated copper and halogen particles. This process requires from 20  $\mu$ sec to several msec in laboratory copper iodide lasers, depending upon the buffer gas pressure and copper halide density. Thus the original laser medium is reconstituted shortly after laser excitation and emission, without loss of material.

Curve 658776-A

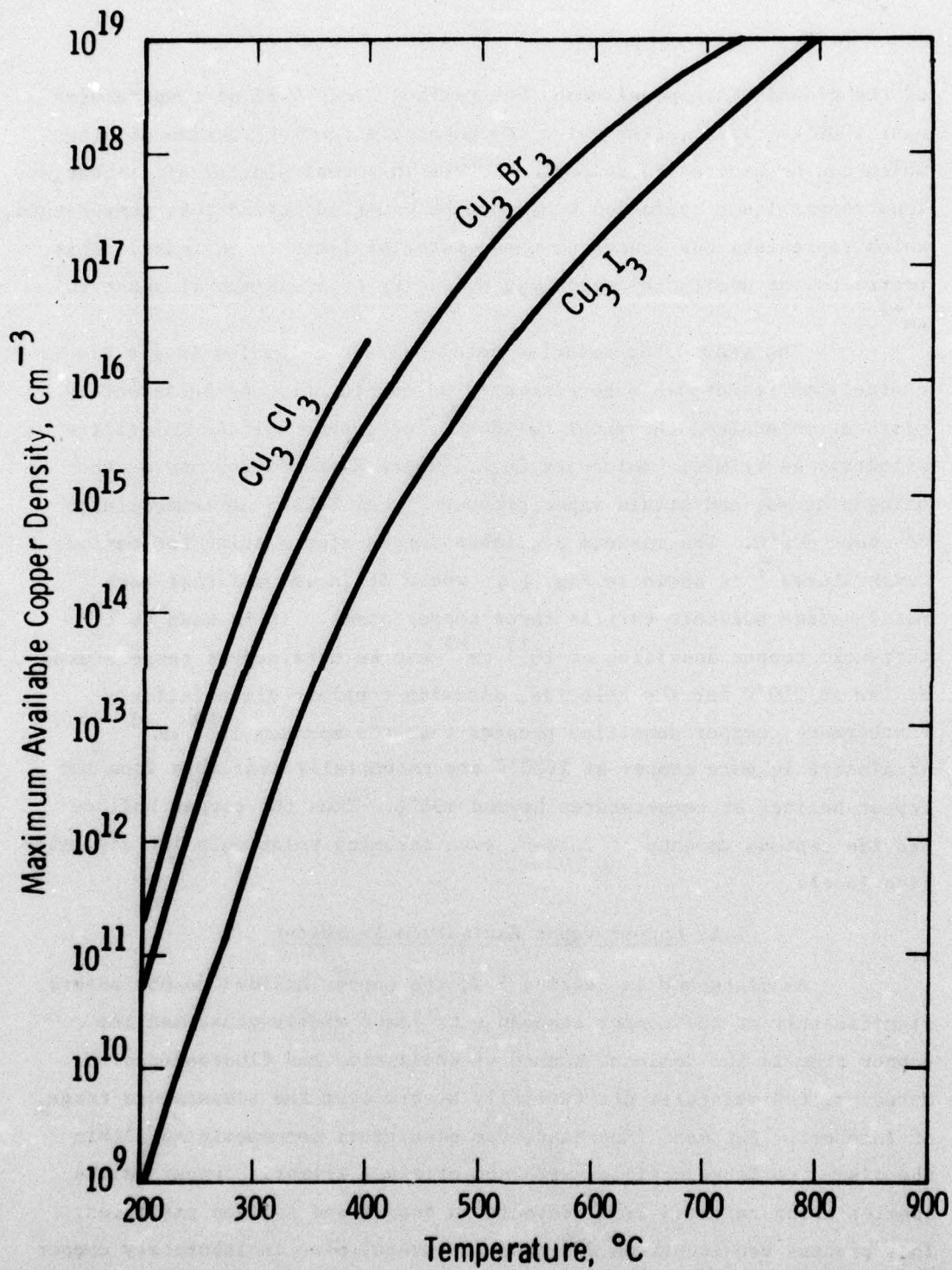


Fig. 1.4—Maximum available copper atom density as a function of temperature for various trimetic copper halides

The short lifetimes of the  $4p^2P_{3/2}$  and  $4p^2P_{1/2}$  upper laser levels in copper require rapid electrical pumping rates to achieve population inversion. Without resonance radiation trapping, this pumping rate must compensate for 10 nsec spontaneous emission losses from these levels; above  $\sim 10^{13} \text{ cm}^{-3}$  copper densities, radiation trapping reduces the resonance level lifetimes to 400-600 nsec.<sup>11</sup> Additionally, any electrical pumping after self-termination of the laser pulse is wasteful. Thus the inherent nature of copper excitation and relaxation kinetics demands rapid electrical pumping of short duration.

The use of copper halides rather than pure copper significantly alters the electrical discharge characteristics of the laser medium. In the first place, dissociation energies of 2.0 to 3.0 eV are required to create free copper atoms from the copper halide vapors.<sup>16</sup> This represents an additional energy loss not present in pure copper discharges, and a potential detractor of the ultimate system efficiency. However this energy investment, like the heat required to vaporize atoms or molecules, can be of negligible proportions provided the copper atoms can be cycled through the electrical excitation process many times before recombination or condensation necessitates a further investment. This suggests high currents and pulse repetition rates to maximize this utilization factor, and low buffer gas pressure to inhibit recombination. Preliminary ground state copper absorption measurements at Westinghouse indicate that recombination times between 20  $\mu\text{sec}$  and 1 msec apply for copper halide Ar discharges with Ar pressures in the 2 to 30 torr range. Thus either double pulsed or high prf operation is suitable for copper halide laser systems.

The second important effect in copper halide discharge is the loss of electrons by attachment to dissociated halogens. The halogens are notoriously electronegative, possessing electron affinities between 2.6 and 2.9 eV.<sup>17</sup> During the rising portion of the current pulse, electron production by ionization exceeds electron loss by attachment, and the electrons are the dominant component of the discharge current. Copper laser excitation, stimulated emission, and self-termination occur during this transient discharge regime, and are little affected by the electron loss process for sufficiently high current levels.

But as the current peaks and declines attachment exceeds ionization, and the current rapidly quenches as electrons disappear and halogen negative ions become the dominant component of the discharge current. As this transition occurs, the discharge E/N passes through that value defined by equal attachment and ionization rates; this condition has been found at Westinghouse to specify the steady-state operating E/N for high pressure CO<sub>2</sub> laser discharges.<sup>18</sup> Thus the principal effect of copper halides upon the discharge characteristics is to increase the effective E/N through greater attachment losses, and to shorten the current pulse duration through accelerated current decline. Both of these tendencies are favorable for increased laser efficiencies. Higher values of the mean electron energy create larger population inversions according to Fig. 1.3, and the shortened current pulse wastes less pumping energy after cessation of the laser emission.

Laser electron attachment losses and the higher values of E/N lead to instabilities which cause the discharge to bow, twist or constrict. Such behavior reduces the excitation volume, deviates the output beam, and can terminate laser action completely when a constricted arc forms. This is a major problem area in copper halide laser discharges, and has frustrated many experimental attempts in the past. More advanced electrode geometries appear to have solved these problems for discharges up to 100 cm in length and about 2.2 cm in diameter. However, as the reservoir temperature is increased the concentration of electronegative species increases, thereby aggravating the discharge stability problem. It appears that discharge instabilities will always present an effective upper limit to the copper halide densities available in diffuse laser discharges.

### 1.5 Laser Energy Output Scaling

Our previous experiments have demonstrated laser output energies of ~3 mJ at energy densities of ~50  $\mu\text{J cm}^{-3}$ . Thus the development of a 50 mJ copper halide laser involves scaling by a factor of 17 beyond present experience. We have developed longitudinal discharge modules that can be scaled in length in a straightforward manner, but scaling

in the radial dimension involves practical difficulties because of discharge stability problems. Two types of scaling approaches have been investigated: (1) energy density scaling and (2) volume scaling.

#### 1.5.1 Energy Density Scaling

If relatively high levels of laser energy density could be tolerated without a significant loss of conversion efficiency due to superradiant losses at 5106 Å, then a relatively straightforward dimension increase would be sufficient to achieve a 50 mJ output. The critical question to be answered is whether this laser energy density and efficiency can be maintained as the tube diameter is scaled up to approximately 3 cm. Superradiant emission losses have been observed to reduce efficiency and energy storage beyond this diameter, and there is great difficulty with discharge stability at high temperatures with larger diameter discharges. However, the scaling to 3 cm diameter does not appear to be unreasonable provided the operating temperature is low, but this in turn degrades the laser specific energy output from  $50 \mu\text{J cm}^{-3}$  to less than  $5 \mu\text{J cm}^{-3}$ . Thus the simultaneous attainment of high laser energy density at large diameters is somewhat frustrated by discharge stability problems which occur at larger diameters.

At low repetition rates ( $\lesssim 1000$  Hz) a double-pulse electrical excitation scheme is required to generate a single laser output pulse in copper halide laser mixtures. If higher repetition rates are acceptable and manageable then increased system efficiencies can be obtained since the dissociation pulse can be eliminated.

#### 1.5.2 Volume Scaling

A straight volume scaling of the discharge up to the 5-liter level will provide a 50 mJ output at  $10 \mu\text{J cm}^{-3}$ . This would require a tube diameter of 5 cm and a total discharge length of 255 cm. The critical question to be answered is whether the required current density, risetime, and discharge stability can be maintained at discharge diameters of 5 cm. While volume scaling is attractive because of its simplicity, it appears that larger diameter discharges suffer from stability and constriction problems in copper halide laser mixtures unless the density

is quite low. Thus the reduced volumetric energy yields which result from lower density operation may not be sufficient to compensate for the larger volumes employed. Volume scaling and energy density scaling are thus interdependent, and the optimum tradeoff between these variables remains somewhat uncertain.

## 2. EXPERIMENTAL RESULTS

### 2.1 Design and Fabrication of High Power Laser Tubes

The laser discharge tubes were fabricated from high quality GE-204 quartz with molybdenum:quartz cup seals serving as electrical feedthroughs. Optical grade quartz windows were fused onto the discharge tube ends at a slightly tilted angle ( $\sim 10^\circ$ ) to avoid internal reflections along the tube axis. Electrodes were made of molybdenum cups with heat shields to improve their thermal efficiency. This type of discharge tube has been operated successfully for over 100 hours without failure under an average power loading of  $50 \text{ W cm}^{-3}$ .

CuBr lasers were excited in either the double pulse or burst mode by a current pulse having ultra-fast risetimes, very short durations and high peak amplitudes ( $>100 \text{ A cm}^{-2}$ ). These required low inductance laser tube designs that minimized circuit inductance.

### 2.2 Design and Fabrication of the Electrical Pulsing Unit

The circuit diagram for the high power pulser is shown in Fig. 2.1. The two capacitors ( $C_d$ ) in series together with the apparent discharge inductance ( $L_d$ ), the stray inductance ( $L_s$ ), and the discharge resistance ( $R_d$ ) form a damped L-C circuit. The characteristic frequency of this circuit is chosen so that one-half of its sinewave is equal to the desired pulse width ( $t_q$ ) of the pulser. All other inductances in the circuit are large compared with  $L_d + L_s$ , so that they have little influence on the discharge circuit while the glow discharge is ignited.

Before the discharge occurs, the two capacitors  $C_d$  are charged to a high positive voltage ( $E_1 = E_2$ ), for instance 10 kV. No voltage potential exists at this time across the discharge to cause ignition. Then at a given time ( $t_1$ ), the hydrogen thyratron ( $Th_1$ ) is triggered, causing its plate to be virtually grounded. This has the effect of suddenly forming a L-C circuit consisting of  $C_{d1}$  and  $L_{r1}$ . Due to the

initial voltage across  $C_{d1}$ , the circuit starts to ring with its own characteristic frequency, say 2 MHz. The result is that the voltage ( $E_1$ ) swings from its original plus 10 kV down past zero toward minus 10 kV (Fig 2.3). If the laser tube were not connected, the voltage difference ( $E_2 - E_1$ ) would reach almost 20 kV. The circuit is often referred to as a "Blumlein Circuit". It provides voltage doubling by what is termed "resonance charging".

If the laser tube is connected as shown in Fig. 2.1 then the glow discharge ignites at some voltage lower than 20 kV (at  $t = t_b$  in Fig. 2.2) and the two capacitors ( $C_d$ ) discharge with a current ( $i_d$ ) through the impedance formed by  $L_d$ ,  $L_s$ , and  $R_d$  with the desired pulse width ( $t_q$ ) as mentioned before, until the glow discharge extinguishes due to insufficient voltage difference left between the capacitors. The thyatron  $Th_1$  extinguishes when the current through it becomes zero.

After this, the two capacitors  $C_d$  recharge again through the charging coil ( $L_B$ ), the diodes (D), and the isolation coils ( $L_1$ ). (The isolation coils are small compared with  $L_B$  and reduce cross talk between the thyatrons.) As long as the charge current keeps the diodes in their conducting state, the charging coil and the parallel combination of the two capacitors, form an L-C circuit, which is tuned to the maximum pulse repetition frequency of the laser. This L-C circuit rings to a voltage which is ideally twice as high as the supply voltage ( $E_B$ ). In this way the circuit accomplishes voltage quadrupling by applying the resonant charging principle twice in series. The diodes avoid a premature discharge of the capacitors once they have attained their maximum voltage.

When the capacitors are fully recharged, the circuit is ready for its next pulse at  $t = t_2$ , which is now initiated through thyatron  $Th_2$  in the same manner as before through  $Th_1$ . This time the discharge current  $i_d$  flows in the opposite direction. Figure 2.3 shows traces from the existing laser driver circuit. The discharge current wave ( $i_d$ ) has a bell-shape rather than half a sinewave because of the non-linearity of  $R_d$ . This circuit has delivered 3 kW to the laser discharge

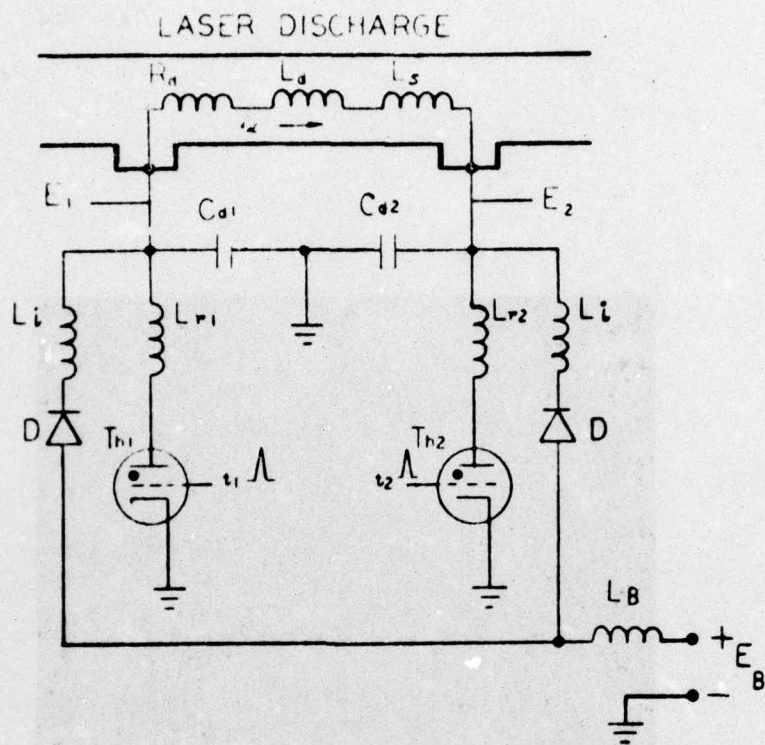


Fig. 2.1 -Basic pulser circuit.

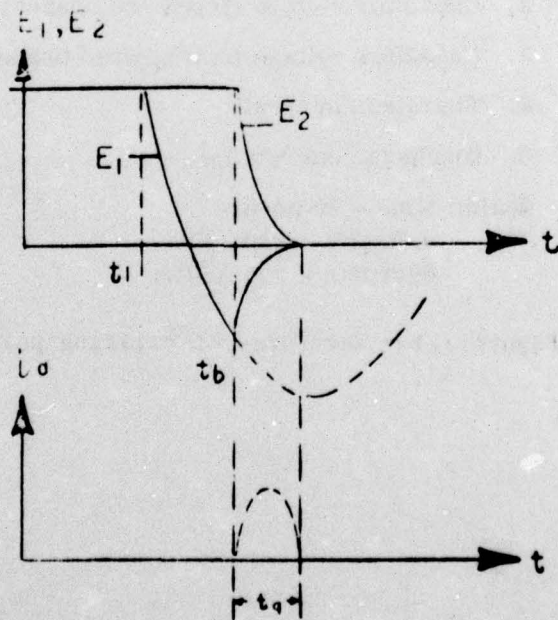
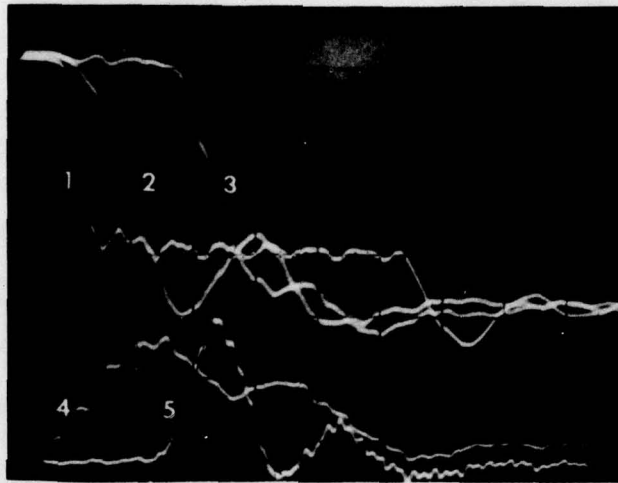


Fig. 2.2- Pulser circuit waveforms.



1. Thyatron plate voltage.
2. Capacitor voltage (triggered branch).
3. Capacitor voltage (untriggered branch).
4. Thyatron current.
5. Discharge current  $i_d$ .

Scale: time - 50 ns/div  
voltages - 5 kV/div  
currents - 100 A/div

Figure 2.3 - Waveforms of existing pulser.

at a pulse repetition frequency of 16 kHz. The capacitors  $C_d$  were charged to 10 kV with a dc power supply voltage  $E_B = 5$  kV. Westinghouse has used this type of circuit repeatedly for military type radars, resulting in a wealth of applicable experience.

Perhaps the prime advantage of these circuits is the fact that the thyratrons are almost isolated from the discharge circuit, once ignition has occurred. This makes it possible to maximize the discharge current slope without concern for the thyatron switching speed.

The Blumlein circuit is well suited to the requirements of the long-lived, high power, variable repetition rate copper halide laser systems. The current reversing feature is important in the continuous operation, since it eliminates problems associated with longitudinal cataphoresis effects<sup>19</sup> and makes possible a truly long-lived, sealed-off laser tube. This pulser can be operated continuously or in a burst mode, and when the burst duration is reduced to allow only two pulses in the burst it becomes a double-pulse power supply with equal energy in the dissociation and excitation pulses. This pulser has been operated at 2.5 kW average power levels and 15 kHz pulse repetition rates for cumulative times exceeding 300 hours without component failure or observable degradation of the operating characteristics. For double pulsed experiments a simplified circuit was employed. This arrangement used separate capacitors for each electrical pulse so that the dissociation and excitation energies could be controlled independently. The capacitors were discharged through triggered spark gaps and the circuits were arranged to minimize inductance and current pulse widths. Thus both double pulse and burst mode excitation could be applied to the experimental discharge tubes, and the separate effects of pulse spacing and relative energy could be varied independently. Long-term multipulse effects could also be observed under burst-mode excitation.

## 2.3 Laser Operating Characteristics

### 2.3.1 Small Bore Tubes

Experimental measurements were made on several laser tubes having a discharge length of 25 cm and a discharge diameter of 0.6 cm. The behavior of these lasers was characterized with respect to variations with halide species, buffer gas species, pressure, input energy and temperature. The lasers were operated in a double pulse mode as a function of time delay between the dissociation and excitation pulses, and in a burst mode as a function of pulse repetition frequency.

Figure 2.4 shows the specific output energy per pulse for a CuBr + 20 Torr He mixture as a function of wall temperature for double-pulse excitation. The tube was operated in an oven so that isothermal conditions were obtained independent of discharge heat dissipation. Optimum operating conditions occur near 530°C, where laser output energy densities of  $45 \mu\text{J cm}^{-3}$  are obtained. Laser emission was observed between  $\sim 450$  and  $650^\circ\text{C}$  for the 25 cm tube. Figure 2.5 shows the specific output energy for the same laser mixture at the optimum temperature as a function of the time interval between the dissociation and excitation pulses. Maximum output occurs for pulse delays near 60  $\mu\text{sec}$ , although laser output is observed from  $\sim 15$  to  $200 \mu\text{sec}$ . A typical output pulse wave form is shown in Figure 2.6.

In measurements using CuCl and CuI halide species the temperature and pulse delay behaviors are essentially reproduced, except that the temperature dependence is shifted somewhat due to the different vapor pressure properties of the chloride, bromide and iodide species. The optimum temperatures for CuCl and CuI are  $\sim 450^\circ\text{C}$  and  $\sim 625^\circ\text{C}$  respectively. There is found to be little dependence of the operating characteristics on buffer gas species. The lighter gases such as He and Ne tend to be better at producing non-constricting discharges, but in sealed-off tubes at operating temperature, He leaks through the quartz wall of the laser tube in very short times ( $\sim 1$  hour). For this reason Ne was used in most measurements. The output energy was found to be only weakly dependent on buffer gas pressure with the maximum output occurring between  $\sim 10$  and  $\sim 20$  Torr.

Curve 689544-A

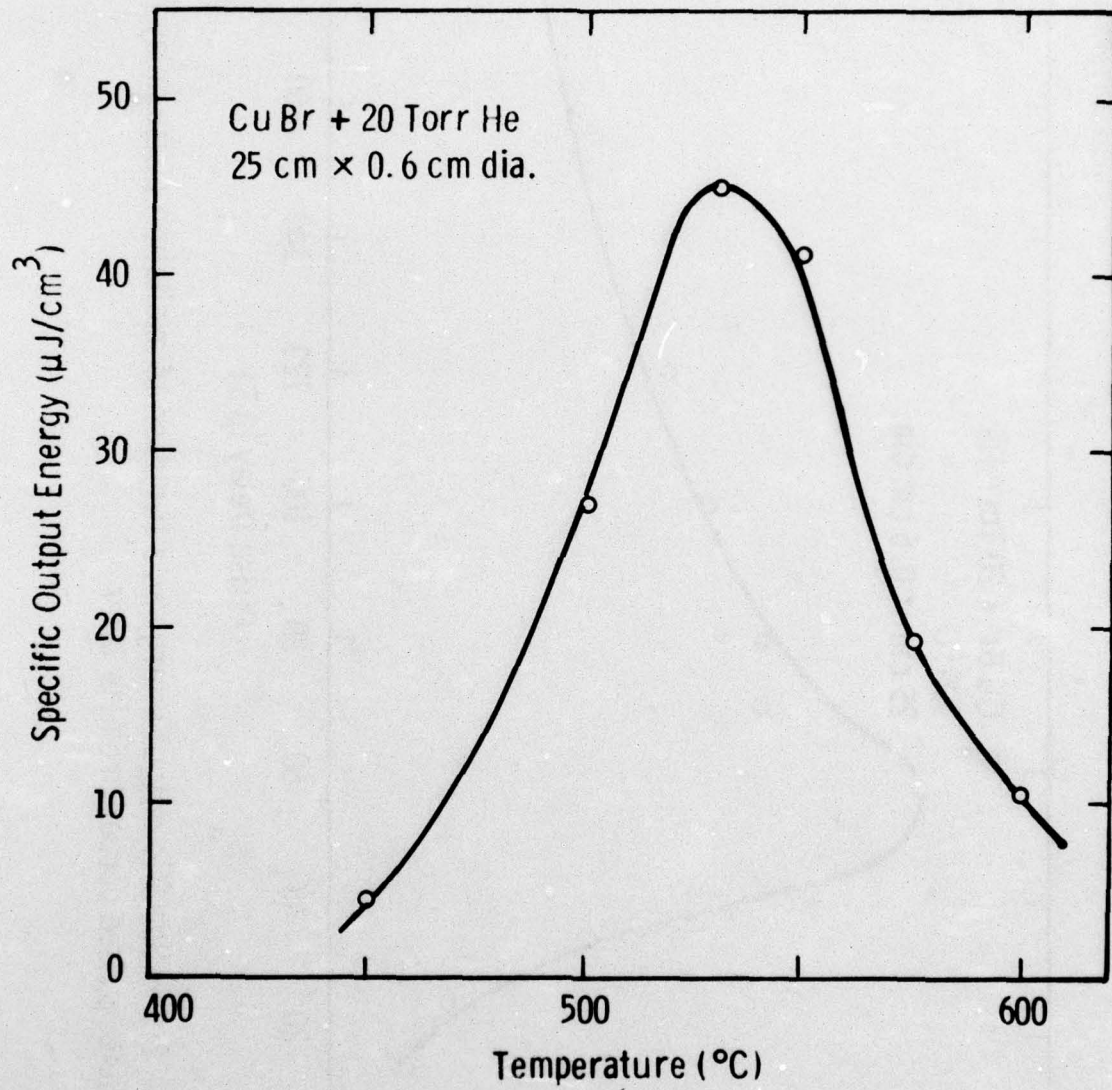


Fig. 2.4 - Specific output energy as a function of wall temperature for a double-pulsed copper bromide laser

Curve 689543-f

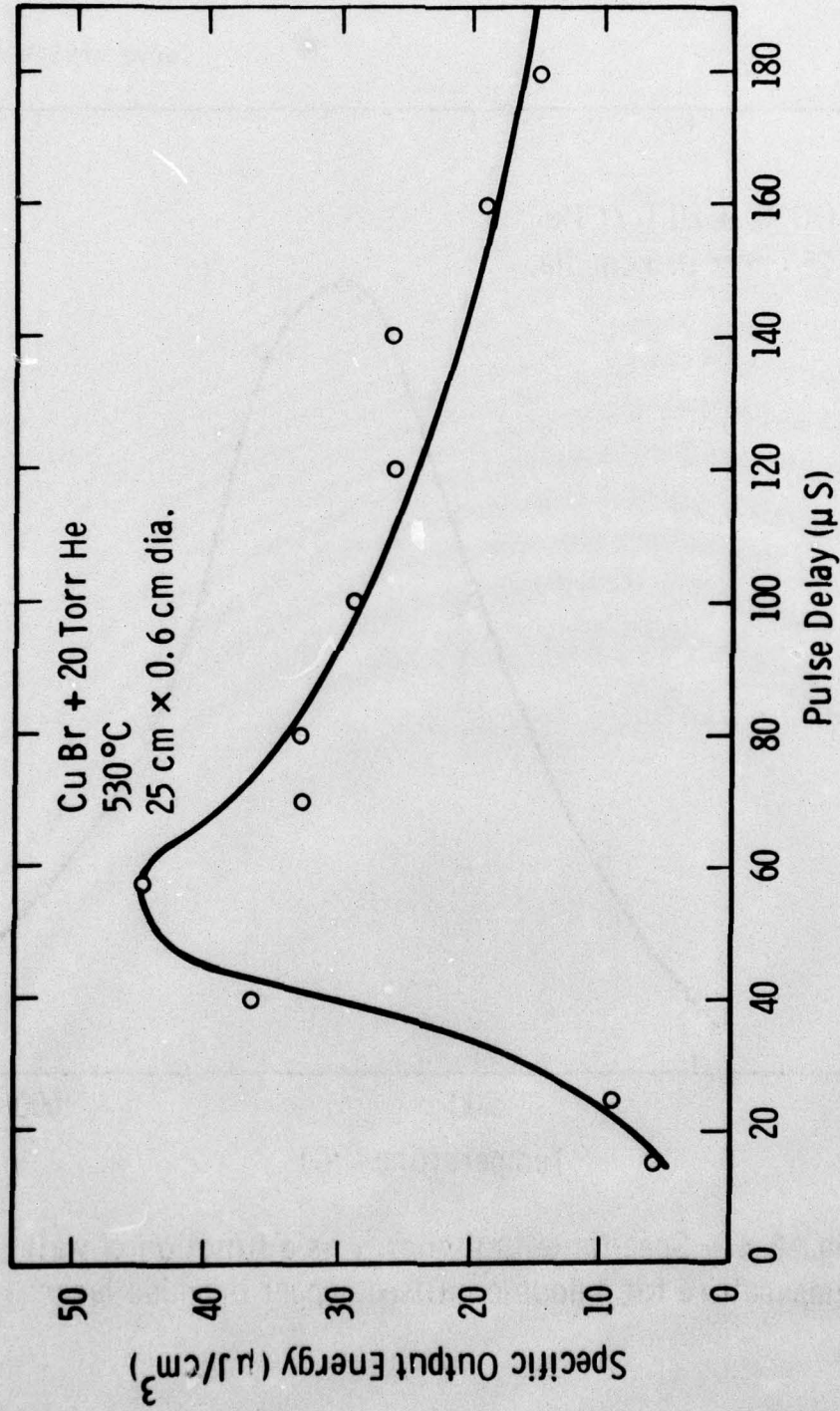


Fig. 2.5 - Specific output energy as a function of excitation pulse delay for a double-pulsed copper bromide laser

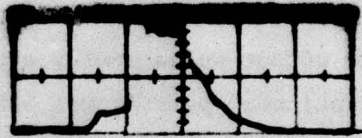


Fig. 2.6. Typical output pulse waveform.

The specific output pulse energy in the double pulse mode was found to be fairly insensitive to the excitation pulse energy over a wide range. Thus the conversion efficiency from electrical energy stored in the excitation capacitor to output energy is highest at low input energy, being .3% at  $14 \text{ mJ/cm}^3$  specific input energy in the excitation pulse. In general, the optimum energy in the dissociation pulse is  $\sim 10$  times that in the excitation pulse.

In the continuous pulsing mode or in burst mode operation, the output pulse energy had dependences on temperature and buffer gas pressure and species which were very similar to those observed in the double pulse experiments. In addition, the optimum pulse repetition frequency corresponded reasonably well to the pulse delay interval of the double pulse measurements for small-bore tubes. The striking difference in behavior between double pulse operation and continuously pulsed operation is in the specific output pulse energy attainable. The greatest value obtained under continuous pulsing was  $\sim 10 \text{ } \mu\text{J/cm}^3$  with a specific input energy of  $10 \text{ mJ/cm}^3$  at a prf of 16.6 kHz. At sufficiently low input powers, the output power was proportional to input power, but saturated at fairly low input levels. The highest efficiency obtained was  $\sim 0.1\%$  under continuous pulsing.

Measurements in a burst mode enable one to see the pulse-by-pulse evolution of the output energy from the first excitation pulse. Our observations indicate that when either the temperature is too low or the input power too high, the output pulse energy decays after an initial rise. Some possible reasons for this behavior will be discussed below; measurements are currently in progress to determine the temporal evolution of the populations of the relevant energy levels through the burst of discharge pulses. The results of these studies should make much clearer the underlying physical causes for the observed multipulse behavior.

### 2.3.2 Large Bore Tubes

Based upon experimental results obtained with small (0.6 cm) bore discharge tubes, attempts were made to scale the dimension of the

discharge region to achieve high energy output pulses. Preliminary measurements in large diameter tubes indicated that severe difficulties would be encountered in producing discharges which completely filled the bore for tube diameters greater than  $\sim 4.0$  cm. Therefore several lasers of more moderate dimensions were operated in both the double pulse and burst modes. Continuous pulsing was also attempted to ascertain average power capabilities. One tube had a discharge length of 50 cm and a bore of 1.2 cm, and a second tube had a discharge length of 100 cm and a bore diameter of 3.0 cm.

Under continuous excitation the 50 cm tube was operated in a self-heated mode using CuBr. The parameters for optimum average power from this tube were very similar to those found for the smaller tubes in burst mode operation, and yielded an average output power of 2 W at a 16 kHz repetition rate with a total input power of 1.5 kW. This corresponds to a specific energy per pulse of  $2.3 \mu\text{J cm}^{-3}$  at an efficiency of 0.13%. The optimum frequency could be varied by altering the magnitude of the input energy per pulse. This effect is shown in Fig. 2.7. Thus one could obtain the same pulse energy at a lower repetition frequency with a corresponding loss of efficiency.

In double-pulsed operation the 50 cm x 1.2 cm tube displayed a temperature dependence which was the same as for the small bore tubes. The optimum temperature was found to be  $\sim 530^\circ\text{C}$ . The dependence of laser output on the time interval between pulses was similar to the smaller tubes, with the optimum delay shifted out to about 150 to 200  $\mu\text{s}$ . However, the specific output pulse energy obtained in the smaller tubes could not be duplicated in the 50 cm x 1.2 cm tube. The best performance obtained was a specific output of  $10 \mu\text{J/cm}^3$  with a delay of  $\sim 200 \mu\text{s}$ . Under these conditions the specific input energies were  $118 \text{ mJ cm}^{-3}$  and  $39 \text{ mJ cm}^{-3}$  respectively for the dissociation and excitation pulses.

The 100 cm x 3.0 cm tube was operated in a burst mode with CuBr, and yielded an output power within the burst of 6.5 W at 16 kHz with an input burst power of 2.2 kW. This corresponds to a specific pulse energy of  $0.57 \mu\text{J cm}^{-3}$  at an efficiency of 0.3%. The operating temperature was much more critical than with smaller tubes, and the

optimum occurred at  $\sim 400^\circ\text{C}$ . At higher temperatures it was not possible to maintain a stable, unconfined glow. This appears to be the crux of the scaling problem; i.e., a large diameter discharge can be maintained only if the density of electron attaching species such as  $\text{Br}_2$  or  $\text{CuBr}$  is low. This, in turn, implies a low gain, low energy density medium.

The 3.0 cm tube was also operated in the double pulse mode, with a wide range of input energies in the dissociation and excitation pulses. The same problem was observed in maintaining a discharge which filled the bore at higher temperatures. The optimum performance was a compromise between  $\text{CuBr}$  density and discharge stability. The best double pulse performance obtained for this tube was a specific output energy of  $2.8 \mu\text{J cm}^{-3}$  at an efficiency of 1.5%.

Table 2.1 summarizes the best observed performance for both double pulse and multiple pulse operation for the three laser discharge tubes described above.

#### 2.4 Absorption Apparatus

The facility used for optical diagnostics of the copper halide laser has been constructed and tested. The spectroscopic apparatus is illustrated in Fig. 2.7. The copper halide laser comprises a longitudinal discharge contained within a high temperature oven. The test laser is operated in "burst" mode. A tunable dye laser which can be externally triggered is employed as a probe source. The transmitted and fluorescence signals are detected through a monochromator by means of a gated photodetector. The detected signals are either displayed on an oscilloscope or are accumulated and stored in a digital multichannel signal averager and processed by a computer through a teletype link. In the foreground of the photograph is the Chromatix CMX-4 dye laser source, and behind this is a shielded box containing the copper halide discharge cell, pulsers and control circuitry. The Fabri-Tek signal average is shown in the rack at the left.

Figure 2.8 depicts the method of absorption measurement. The copper halide discharge is driven by a high voltage pulsed power supply (pulser) which is triggered by a train of pulses generated by

Table 2.1. Summary of Copper Bromide Laser Tube Performance

Quantity	Double Pulse	Multiple Pulse	Double Pulse	Multiple Pulse	Double Pulse	Multiple Pulse	Double Pulse	Multiple Pulse
Diameter, cm	0.6	0.6	1.2	1.2	3.0	3.0	3.0	3.0
Length, cm	25	25	50	50	100	100	100	100
Volume, cm <sup>3</sup>	7.06	7.06	56.5	56.5	706	706	706	706
Optimum Temperature, °C	530	530	530	530	450	400	400	400
Laser Pulse Energy, μJ	318	70.6	565	125	2000	406	406	406
Specific Output Energy Density, μJ cm <sup>-3</sup>	45	10	10	2.3	2.8	0.57	0.57	0.57
Optimum Pulse Interval, μsec	60	--	200	--	250-300	--	--	--
Optimum prf, kHz	--	16	--	16	--	16	--	16
Laser Output Power, W	--	1.1	--	2.0	--	6.5	--	6.5
Efficiency, %	0.3*	0.1	1.0*	0.13	1.5*	0.3	1.5*	0.3

\* Includes only the excitation pulse energy.

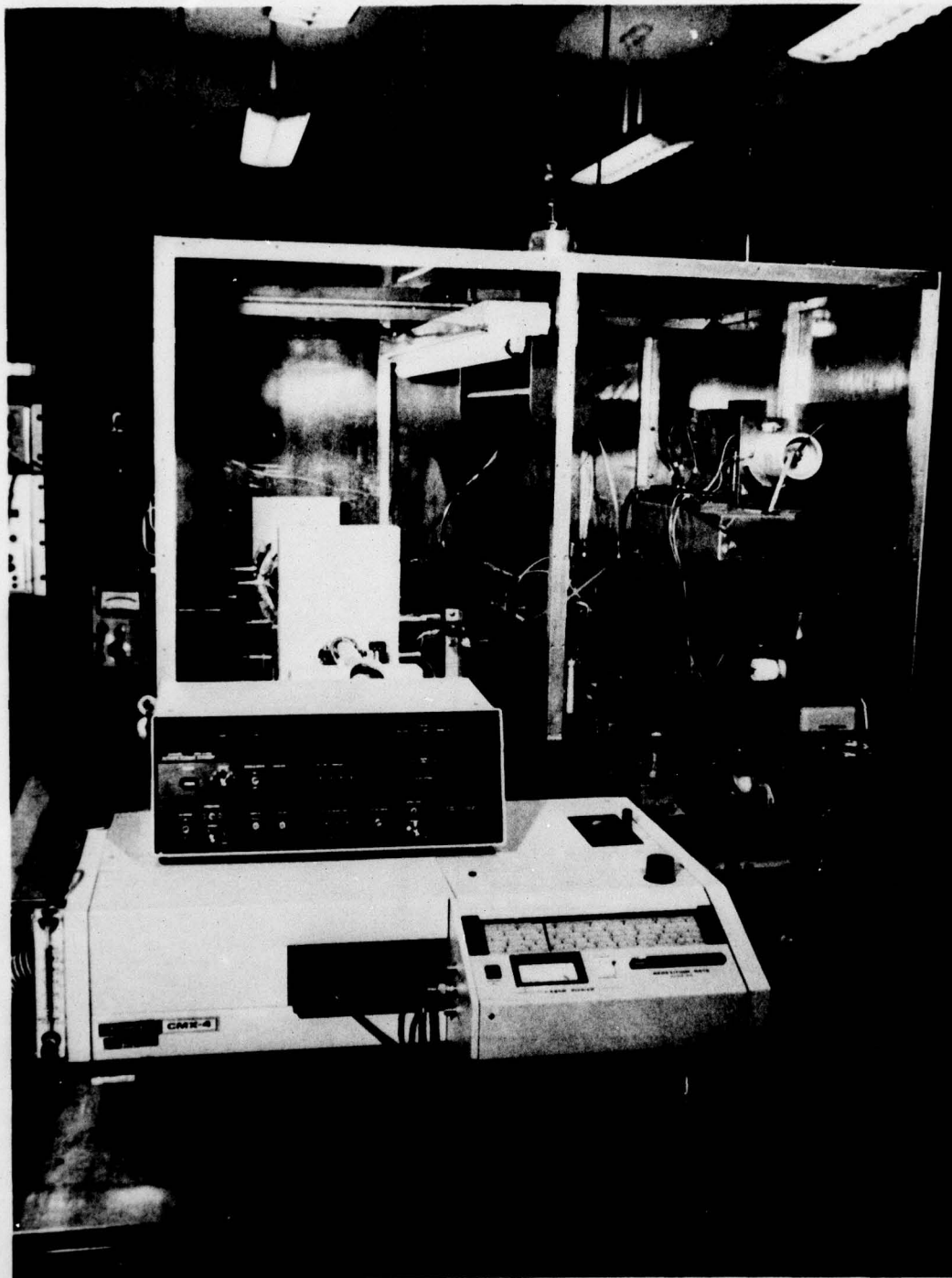


Figure 2.7—Experimental absorption apparatus showing the dye laser source, absorption cell container, and multichannel signal averager.



an American Electronics Laboratory Model 138 pulse generator. The pulse repetition rate and pulse train duration can be varied. A typical train may consist of pulses approximately 100  $\mu$ s apart with an over-all burst duration of 10 ms. Under these conditions, each burst consists of 100 pulses. The pulse trains are separated by 100 ms in order to (a) maintain the laser at approximately the same temperature from burst to burst and (b) keep the burst repetition rate within the permissible repetition rate of the tunable dye laser probe.

The probe laser is a Chromatix CMX-4 tunable dye laser. This laser is designed to fire only at the peak of the 60 cycle sine wave of the line frequency. The clock that provided the timing pulses for both the dye laser and the copper laser is the trigger output of a Tektronix oscilloscope, synchronized to the line frequency, thereby assuring minimum jitter between the firing of the probe laser and of the copper laser. A computer program which included line shape overlap to unfold the absorption measurement has been written and debugged.

## 2.5 Lifetime Limitations and Tube Configurations

There are two features of the copper halide laser system which might eventually limit the operating lifetime, namely the switching thyratrons and  $\text{Cu}^+$  diffusion into the quartz envelope. By using the double-Blumlein circuit described previously, we have life tested the pulser cumulatively for over 300 hours ( $>10^{10}$  shots) without any failure. According to chemical analysis of a 50-hour laser tube, no actual chemical reaction had taken place inside the laser tube, except for copper diffusion and electrode sputtering. Without any modification, the present copper halide laser system should be able to operate beyond 500 hours. The operating lifetimes of electrodes can be improved by using more effective heat shields or more efficient electron emitters.

### 3.0 CONCLUSIONS AND RECOMMENDATIONS

The properties of double-pulse and multipulse copper halide lasers have been established by the fabrication and experimental testing of three quartz discharge tubes. These tubes were operated as all-hot, sealed-off systems contained within temperature-controlled ovens for double-pulse and burst-mode excitation, and as self-heated systems for continuously-applied pulsed electrical excitation. Both pulser and tube designs have demonstrated reliable operation under high power, high prf operation: pulser lifetimes of 300 hours and laser tube lifetimes of 100 hours without failure have been recorded for self-heated, high power operation. The purpose of this present study was to assess the applicability of these laser technologies to the high pulse energy regime of interest for Navy applications.

The principle conclusion of this study is that high energy operation is presently inhibited by discharge stability problems which occur in scaled-up laser discharge tubes. When the tube diameter is small as in the 0.6 cm diameter tests, specific output energies of  $45 \mu\text{J cm}^{-3}$  can be obtained routinely under double-pulse excitation. This performance is reduced to  $\sim 10 \mu\text{J cm}^{-3}$  under multipulse excitation due to cumulative effects which are qualitatively understood as originating from gas heating and radial cataphoresis. These cumulative multipulse effects can be reduced substantially with more advanced discharge tube designs, but for the present longitudinal discharge configurations such effects limit the maximum available specific energy density in multiply-pulsed excitation schemes. Nonetheless, these levels of performance are more than adequate to contemplate the design of high output energy lasers.

As the tube diameter is scaled up to 3.0 cm a systematic decrease in the specific laser energy density is experienced. At 1.2 cm tube diameter the double-pulse output drops to  $10 \mu\text{J cm}^{-3}$ , and at 3.0

cm the double-pulse output is  $2.8 \mu\text{J cm}^{-3}$ . In each case the discharge length consisted of 25 cm segments connected in tandem, so discharge current magnitudes and risetimes remained approximately constant even though the total discharge lengths differed. A similar reduction in multipulse outputs was observed with increases in tube diameter. The derating factor from double to multiple pulsing was approximately 5 for the tubes studied. Thus increasing the tube diameter decreases the specific output energy in a nonlinear fashion for both double and multiple pulsing.

This inverse relationship between specific output energy and diameter is easily correlated with discharge stability problems. At the larger diameters the discharge does not completely fill the tube cross section, and at 3.0 cm diameter the optimum double-pulse operation occurs at temperatures of  $450^\circ\text{C}$ . At higher temperatures the discharge breaks into constricted filaments, presumably due to higher levels of electro-negative discharge species. Evidently the larger diameter tubes are simply less tolerant of electron attachment losses which occur at higher temperatures. Thus discharge stability considerations force lower operating temperatures in large diameter tubes. Since the copper bromide vapor pressure is very sensitive to the temperature reduction from  $530^\circ\text{C}$  to  $450^\circ\text{C}$ , the vapor pressure is reduced substantially and the laser operated very close to threshold. As demonstrated in the laser output data presented in Fig. 2.4 for the 0.6 cm tube, a reduction in wall temperature from  $530^\circ\text{C}$  to  $450^\circ\text{C}$  is sufficient to reduce the specific output energy from its optimum of  $45 \mu\text{J cm}^{-3}$  to a near-threshold level of  $\sim 4.5 \mu\text{J cm}^{-3}$ , a factor of 10 reduction. The remaining factor accounting for the observed  $2.8 \mu\text{J cm}^{-3}$  is likely the lack of discharge filling at the 3.0 cm tube diameter. Thus discharge stability problems force near-threshold laser operation, and the discharge fails to fill the available aperture as the diameter is scaled to 3.0 cm. These effects account for the reduced laser performance as the diameter is scaled.

As the specific output energy declined with tube diameter, the laser conversion efficiency improved for both double and multiply

pulsed excitation. The explanation for this behavior is not immediately evident, but is likely related to the reduced gas discharge heating per unit volume which occurs at the larger diameters. Alternatively, the larger tube diameters require longer intervals between successive pulses for optimum output, indicating that the laser kinetics of copper ground state and metastable destruction rates are more favorable at these larger tube diameters. Whatever the explanation, it appears that the specific output energy and the laser conversion efficiency bear an inverse relationship to one another as the tube diameter is varied.

It is important to note that the optimum prf for multipulse excitation does not vary with tube diameter over the range studied, even though the optimum pulse energy for double-pulse excitation does increase monotonically with increasing tube diameters. It appears that the multipulse excitation of copper halide lasers involves cumulative kinetic effects which render the optimum time between pulses independent of wall effects. Volume deexcitation of copper metastables by gas collisions is a likely explanation for this observation. Thus it is seen that as the tube diameter increases and specific output laser pulse energy decreases, the average laser output power increases with tube diameter since the optimum prf remains constant. Furthermore, laser properties appear to be scalable in terms of discharge length in a straightforward manner. This implies that the volume scaling of copper halide lasers provides attractive increases in the average power output at high prfs, and also improves the operating efficiency of the laser system.

Copper halide lasers do not scale attractively in specific energy output as the diameter increases, but the efficiency improves significantly. The limitation is discharge stability, and it is important to observe that the small diameter results clearly show that high specific output energies are indeed available from copper halide lasers. Thus the heart of the matter is discharge stability. If this problem can be overcome, then copper halide lasers will have attractive energy scaling laws.

This study recommends two principle future directions for further activities in copper halide lasers. The first is to recognize

the inherent advantages of copper halide lasers at high prfs under continuously-pulsed, self-heated conditions, where the length, diameter and prf scaling laws are very attractive for average power and efficiency. These features, coupled with the demonstrated sealed-off, long-lived tube characteristics, render the copper halide laser especially attractive for applications where reliable, high prf, high average power laser sources are required. Evidently the low prf, high energy regime does not favor the best operating features of these lasers.

The second recommendation is that practical solutions to the discharge stability problem in copper halide lasers should be developed in order to realize the full promise of high specific output energies in larger tube embodiments. Various forms of transverse discharges offer considerable promise for solving this problem. Of course, the technological difficulties of high temperature operation in such discharge configurations are considerable. However, the laser performance improvements to be realized by overcoming discharge stability limitations are substantial.

#### 4. REFERENCES

1. W. T. Walter, M. Piltch, N. Solimene, and G. Gould, *Bull. Am. Phys. Soc.*, 11:113 (1966).
2. W. T. Walter, M. Piltch, N. Solimene, and G. Gould, *IEEE J. Quant. Electr.*, QE-2:474 (1966).
3. W. T. Walter, *IEEE J. Quant. Electr.*, QE-4:355 (1968).
4. A. A. Isaev, M. A. Kazaryan, and G. G. Petrash, *JETP Letters*, 16:27 (1972).
5. G. R. Russell, N. M. Nerheim, and T. J. Pivrotto, *Appl. Phys. Letters*, 21:565 (1972).
6. ONR Contract N000-14-73-C-0317 (unpublished).
7. AFWL Contract F29601-72-C-0079 (unpublished).
8. T. S. Fahlen, Paper S-10, Eighth International Quantum Electronics Conference, San Francisco, California, June 10-13, 1974.
9. L. A. Weaver, C. S. Liu, and E. W. Sucof, *IEEE J. Quant. Electr.*, QE-9:645 (1973).
10. C. S. Liu, E. W. Sucof, and L. A. Weaver, *Appl. Phys. Letters*, 23:92 (1973).
11. L. A. Weaver, C. S. Liu, and E. W. Sucof, *IEEE J. Quant. Electr.*, QE-10:140 (1974).
12. C. J. Chen, N. M. Nerheim, and G. R. Russell, *Appl. Phys. Letters*, 23:514 (1973).
13. I. Liberman, R. V. Babcock, C. S. Liu, T. V. George, and L. A. Weaver, *Appl. Phys. Letters*, 25:334 (1974).
14. C. E. Moore, Atomic Energy Levels, Vol. II, p. 111, Circular of the Nat. BuStd., 467 (1952).

15. R. A. J. Shelton, *Trans. Faraday Soc.*, 57:2113 (1961).
16. A. G. Gaydon, *Dissociation Energies and Spectra of Diatomic Molecules*, Second Edition, Chapman and Hall, p. 224, 1953.
17. J. J. DeCorpo and J. L. Franklin, *J. Chem. Phys.*, 54:1885 (1971).
18. L. J. Denes and J. J. Lowke, *Appl. Phys. Letters*, 23:130 (1973).
19. C. S. Liu, D. W. Feldman, J. L. Pack, and L. A. Weaver, *J. Appl. Phys.*, 48:1 (January 1977).